

The crystal structure of stilpnomelane. Part III: Chemistry and physical properties

R. A. EGGLETON AND B. W. CHAPPELL

Department of Geology, Australian National University, Canberra, A.C.T.

SUMMARY. Full chemical analysis, cell dimensions, γ refractive index, density, and infra-red absorption spectrum have been determined for fourteen stilpnomelanes. Coupled with data from previously described material and electron probe analyses of three further samples, the new information shows that $\gamma = 1.616 + 0.0047 \text{ Fe}^{3+} - 0.0037 \text{ Mg}$; substitution of Mn for Fe appears to have little effect on γ . For ferrostilpnomelane, $D = 2.85 - 0.011 \text{ Mg}$, for ferristilpnomelane, $D = 2.89 - 0.011 \text{ Mg}$. Cell dimensions clearly distinguish ferro-, ferri-, and manganstilpnomelanes; for ferri-stilpnomelane $a = 22.03 - 0.00446 \text{ Mg} - 0.00786 \text{ Fe}^{3+}$ (Å). A convenient approximation to the structural formula using a $\frac{1}{8}$ subcell, is $\text{K}_{0.6}(\text{Mg}, \text{Fe}^{2+}, \text{Fe}^{3+})_6\text{Si}_8\text{Al}(\text{O}, \text{OH})_{27} 2-4 \text{ H}_2\text{O}$.

STILPNOMELANE is unique among layer silicates in accommodating a wide range of oxidation state of iron without major structural change (Eggleton and Bailey, 1965; Eggleton, 1972). This property, coupled with its large triclinic unit cell, leads to a complex structural formula, which in an ideal, pure iron, ferrostilpnomelane might be represented as $\text{K}_5\text{Fe}_4^{2+}[\text{Si}_{16.3}\text{Al}_9]\text{O}_{16.8}(\text{OH})_{4.8} \cdot 12\text{H}_2\text{O}$. Oxidation is accompanied by the conversion of (OH) to O, giving an extreme ferristilpnomelane composition $\text{K}_5\text{Fe}_3^{2+}[\text{Si}_{16.3}\text{Al}_9]\text{O}_{21.6} \cdot 36\text{H}_2\text{O}$. Neither extreme has been reported. This variation in stilpnomelane composition, as well as the substitution of Mg and Mn for Fe, produce variations of cell dimensions, refractive index, and density; the relation between these is reported here.

Sample descriptions. Stilpnomelane occurs in a variety of geological environments, and specimens have been selected from as many of these as possible (Table I, p. M37). Some of the material used was described in Part II, and these samples bear the same designation as in Part II.

1. Stilpnomelanes from greenschists: Samples B, C, L, P, Q, V, are from the New Zealand Otago schists, and are similar, in some cases almost identical to those described by Hutton (1938). Sample D is from British Columbia (Read, 1973); R and W from the Coast Ranges, California.

2. Stilpnomelanes from iron deposits: Samples A, F, G, H, I, and J are from the Lake Superior Precambrian Iron Formations, sample M from the Hamersley Ranges, Western Australia, N and O from Grythytte, Sweden.

3. Stilpnomelanes from metal sulphide deposits: Samples E, S, T, U, X, Y are from the Great Cobar (N.S.W.) Mine, associated with magnetite, chlorite, quartz, pyrrhotine, and chalcopyrite. The Cobar occurrence was described by Rayner (1961) and his analysis is listed in Part II (analysis 21). New samples were collected from drill core and from the Great Cobar mine dump, in the hope that primary variation in $\text{Fe}^{3+}/\text{Fe}^{2+}$ ratio might be related to associated mineralogy and indirectly to oxygen fugacity inferred from such mineral pairs as pyrite-pyrrhotine, or quartz-magnetite. It was found, however, that the $\text{Fe}^{3+}/\text{Fe}^{2+}$ ratio related to the grain size and the length of time the core has lain in the core yard (between 1 and 12 years). Analyses were made of 4 Cobar stilpnomelanes; except for $\text{Fe}^{2+}/\text{Fe}^{3+}$ ratio the analyses are essentially identical (E, S, T, U). Variations in the physical properties of these samples can therefore be related to $\text{Fe}^{2+}/\text{Fe}^{3+}$ only (see, for example, the 6 Cobar samples in fig. 3).

4. Stilpnomelanes from the weathering profile: Most of the ferristilpnomelanes listed in Part II were recognized by their respective investigators as surface oxidized ferrostilpnomelane. Klein (1974) describes adjacent brown and green stilpnomelane from iron formation, and concludes that the dissimilar $\text{Fe}^{3+}/\text{Fe}^{2+}$ ratios are primary, not the result of weathering. There are few other suggestions in the literature that ferristilpnomelane is ever a natural primary phase. In a skarn, 12 km north of Canberra, in the Australian Capital Territory hedenbergite pyroxene weathers to the smectite nontronite, which in turn breaks down to ferristilpnomelane. This process is clearly visible in thin section (fig. 1) where colourless hedenbergite is

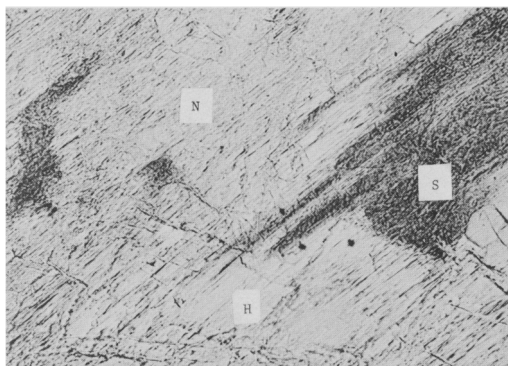


FIG. 1. Formation of stilpnomelane from nontronite after hedenbergite.

topotaxially replaced by yellow nontronite, which is in turn replaced by a random aggregate of brown ferristilpnomelane.

The iron in the hedenbergite is all ferrous, that in the nontronite all ferric (Eggleton, 1975), and that in the stilpnomelane (Sample Z) inferred ferric from cell dimensions and colour. It is inconceivable that the stilpnomelane in this occurrence was ever ferrostilpnomelane; the field evidence allows only the interpretation that the stilpnomelane has crystallized under surface atmospheric oxidizing conditions from nontronite.

Chemistry and structural formulae. Analyses of the stilpnomelanes are given in Table I (p. M37). Sodium was determined by flame photometry. Other metal cations and sodium were measured by X-ray spectrometric analysis of a fused sample using the method of Norrish and Hutton (1969). Difficulties in measurement of satisfactory H_2O contents prompted a variety of approaches to the analysis of that component. Initial measurements were made by heating in air in a combustion tube at $1200^\circ C$ and collecting H_2O in a P_2O_5 -filled absorption tube, following Riley (1958). Data obtained were poor and the analyses totals unacceptably low. The analysis of H_2O in Fe^{2+} -bearing sheet silicates is difficult because of redox reactions. More satisfactory results were obtained when a lead oxide-lead chromate flux (Peck, 1964) was added to the sample prior to ignition.

The bulk of the water analyses in Table I were made by Marcelyn Cremer of the U.S. Geological Survey. The Penfield method (Peck, 1964) was used for samples C, E, P, U, and W and a microcoulometric technique (Cremer and Elsheimer, 1972) for samples J, O, Q, and V. In both these techniques, the sample is fluxed in an attempt to eliminate redox reactions and consequent water loss. Despite this, most of the analyses have totals that would normally be regarded as unsatisfactory. We ascribe

this to low water values, probably caused by oxidation of Fe^{2+} by water at low temperatures prior to oxidation by the flux.

FeO was determined by dissolution in $HF-H_2SO_4$ mix followed by titration with potassium dichromate (Peck, 1964).

Structural formulae have been calculated using the measured cell volume and density. Because this method does not assume a 'correct' anion total, no error in cation cell content is introduced by the problems in water analysis. We accept that the low analytical total is solely caused by undetected H. The averages and ranges for tetrahedral Si and Al are not significantly different from those listed in Part II. Octahedral Al is slightly less (1.0 compared with 2.3), and the range of Mg slightly extended compared with Part II. The total octahedral $Al+Fe+Mn+Mg$ of 46.8 is one less than the structural maximum of 48; the coefficient of variation (1.4%) is about the same as the estimated experimental error in density measurement.

In Part II, it was postulated, for structural reasons, that no more than thirty trivalent ions could occur in the octahedral sheet of ferristilpnomelane. After heating sample T to 200° for 48 hours, only 1.4% FeO remained, equivalent to an octahedral sheet content of about $41 R^{3+}$. Under the same conditions, sample N retained 2.5% FeO , results comparable with those of Nitsch (1970) who found 2.9% FeO in experimental studies.

It is clear that under suitably oxidizing conditions, considerably more than $30 R^{3+}$ can occur in the octahedral layer (see also analyses A and Z) but there may none the less be a limit. Biotite with the same initial FeO as sample T showed no significant change in FeO after heating to 200° . There are only six octahedra in stilpnomelane having the environment of those in biotite (connected to four Si tetrahedra symmetrically, with the (OH) at opposite apices of the octahedron), and possibly iron in these six octahedra cannot be oxidized.

The total of $4.8 Ca+Na+K$ is essentially the same as listed in Part II. There are two small and three large cavities in the interlayer where a large cation might rest (fig. 2), and we postulate that these five cations occur in these positions. The bonding in three of these sites (marked B in fig. 2) is particularly weak, as the apical oxygens of the inverted tetrahedra are about 4 \AA from the cavity centre. It is presumably from these sites that the potassium migrates under electron-beam heating (Graham, 1976).

The large cations account for all but about -3 of the tetrahedral sheet charge deficiency caused by substitution of Si by Al. The difference appears to be made up in the octahedral sheet, as in biotite,

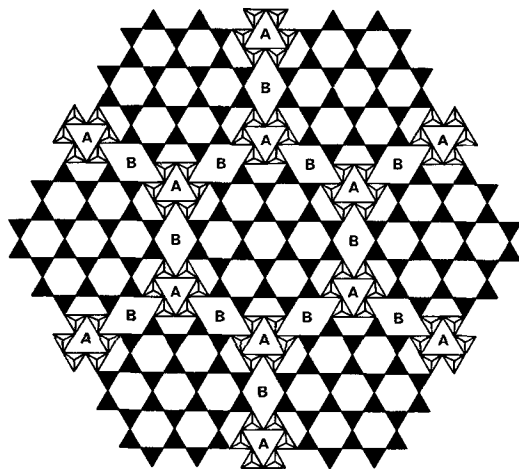


FIG. 2. Positions for large cations in the stilpnomelane tetrahedral sheet. Sites A are inside a cage of tetrahedra, B are more open.

where the tetrahedral deficiency exceeds the inter-layer cation charge by more than 0.5 per eight tetrahedral sites (Deer *et al.*, 1962), equivalent to a difference of more than -4 per 72 stilpnomelane tetrahedral sites.

As in Part II, we allocate sufficient H as (OH) in the octahedral layer to balance the overall charge, but we do not here distinguish H balancing octahedral charge from that to balance the tetrahedral deficiency (distinguished as (OH)⁻ and H⁺ in Part II). The remaining H is allocated as H₂O. Total H (= 72) is lower than the average listed in Part II (= 79), presumably from failure to oxidize all H during water analysis.

TiO₂, P₂O₅, and CO₂ are all low, and have been neglected in calculating structural formulae.

Cell dimensions. The triclinic unit cell of stilpnomelane is large and unwieldy, however, because it is pseudo-trigonal, only the edge *a* and thickness (*d*₀₀₁) of the pseudo-trigonal cell are needed to calculate the other cell parameters. Their measurement is described in Part II.

Attempts to relate cell dimensions precisely to composition are self-defeating because of the inevitable range of oxidation state shown by one sample. Both *a* and *d*₀₀₁ vary with Fe³⁺ content,

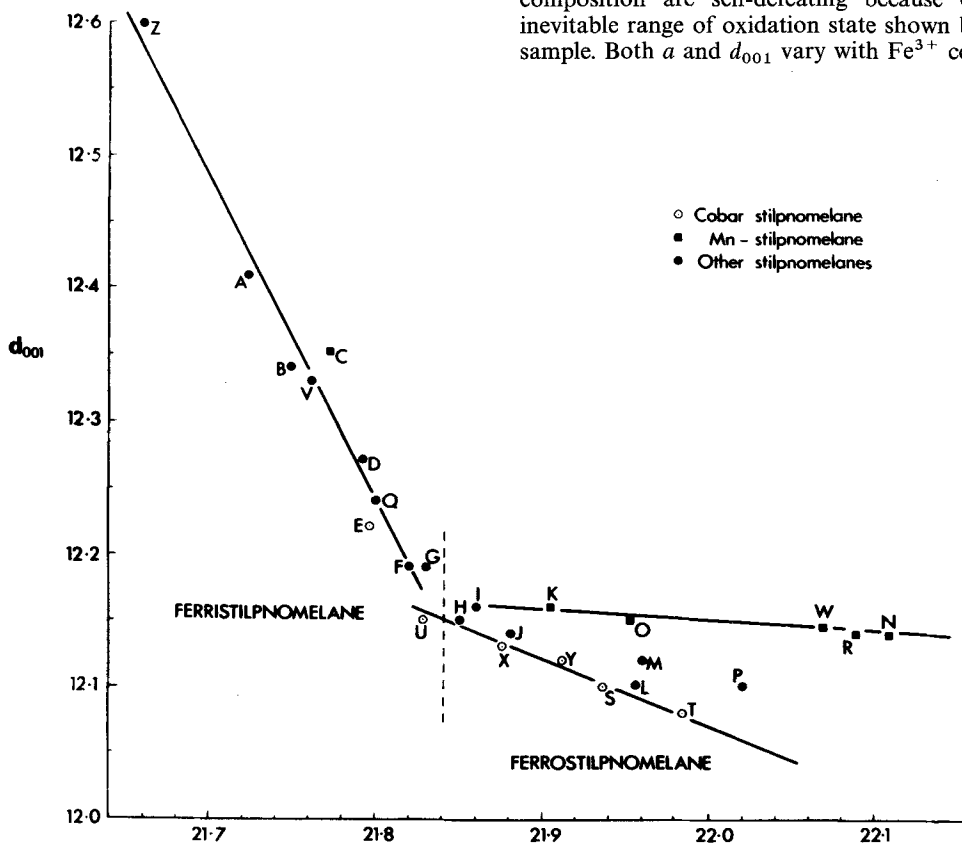


FIG. 3. *a* vs *d*₀₀₁ for stilpnomelane.

thus a powder photograph taken using a well-mixed sample gives broad lines. A sharp photograph can be obtained by crushing a single flake, but this flake cannot represent the analysed material. The data plotted in fig. 3 are cell dimensions determined from single flakes. The regions of ferristilpnomelane ($\text{Fe}^3/\text{Fe}^2 > 1$), ferrostilpnomelane, and manganiferous ferrostilpnomelanes (ekmanites, Matkovsky, 1964, Shirozu, 1964) are clearly separated. For the eleven samples A, B, C, D, E, F, G, Q, U, V, Z, a (\AA) = $22.03 - 0.00446 \text{ Mg} - 0.00786 \text{ Fe}^{3+}$, correlation = 0.91. For the ferrostilpnomelanes, no satisfactory regressions can be established between cell parameter and composition. In fig. 3, the low-magnesium Cobar samples S, T, U, X, Y, the three high magnesium samples J, M, P, and the five manganiferous ferrostilpnomelanes K, N, O, R, W, each define linear trends, but the data do not permit the establishment of more precise relations.

Refractive index. Only the γ index has been determined for these samples. For all samples the perfect cleavage prevented the formation of an edge suitable for the production of a normal Becke line, and so the relative indices of grain and oil were determined by oblique illumination. This reduces the accuracy of these measurements to ± 0.002 for $\gamma < 1.7$, ± 0.005 for $\gamma > 1.7$. For some samples (R, Q) the index range exceeds this accuracy.

Existing graphs relating refractive index to composition ascribe Fe^{3+} as the only variable, and the data points scatter fairly widely (see for example, Deer *et al.*, 3, Fig. 26). The scatter is caused largely by variation in Mg content, as can be seen from fig. 4, where γ is plotted against Fe^{3+} cations. Lines of equal magnesium content calculated by linear regression for 2 variables are drawn at intervals of 5 Mg cations, and the Mg content of each sample is given for comparison. Samples R and Q have a range of refractive indices and are not plotted. For the remaining samples, $\gamma = 1.616 + 0.0047\text{Fe}^{3+} - 0.0037\text{Mg}$. Given a figure for Mg this relation predicts well the ferric iron octahedral sheet composition for most stilpnomelanes of Part II for which a γ -index was reported by the original author (Table II, p. M37). As with the cell dimensions, the range of oxidation state of iron in a sample prevents index measurements from being truly representative of the material analysed. In addition, the regression coefficients have been calculated ignoring Al, Mn, and octahedral vacancies, as well as the larger cations and water, so the equation cannot be expected to be exact.

Refractive index γ is plotted against a in fig. 5. Lines of equal magnesium content have been positioned by eye, with slopes determined from reduced and oxidized samples from the same rock. The lines of equal ferric iron have been positioned

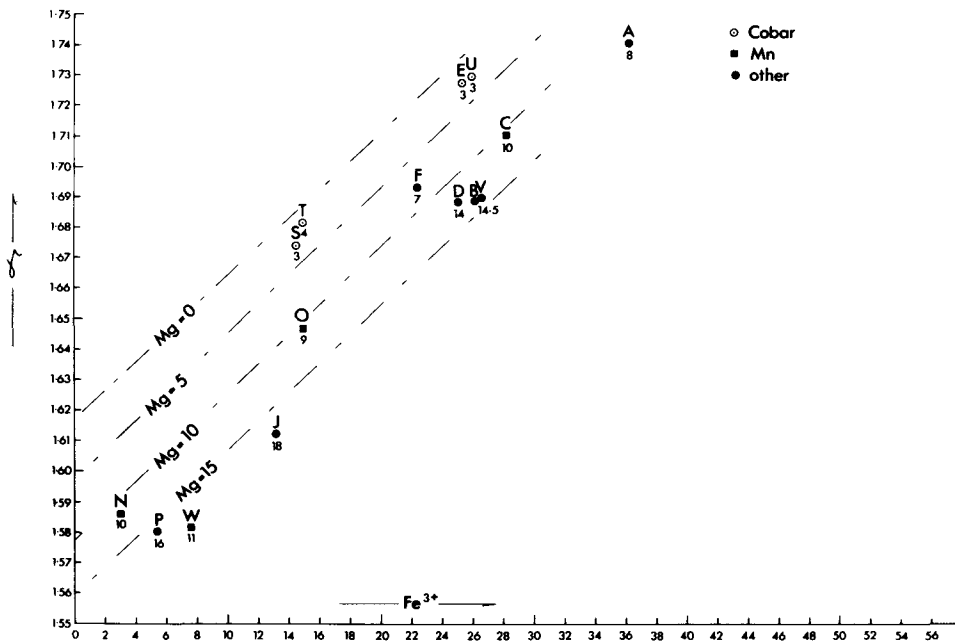


FIG. 4. Variation in γ refractive index with composition. Subscripts to symbols are magnesium content per forty-eight octahedral cations.

365

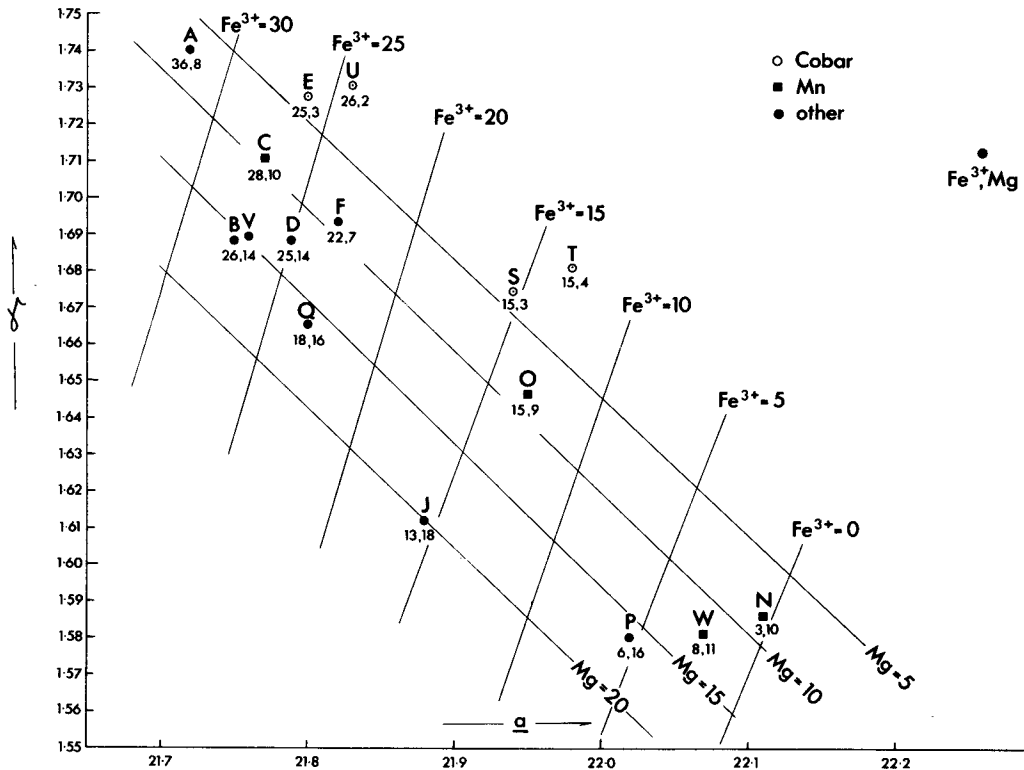


FIG. 5. Relation between a cell-edge, γ refractive index, and octahedral layer composition.

by using fig. 4. For an unknown stilpnomelane, figures 3, 4, and 5 allow an approximate composition to be determined from cell dimensions and γ -refractive index. Where an electron-probe analysis is also available, the $\text{Fe}^{2+}/\text{Fe}^{3+}$ ratio can be determined with more certainty.

Density. Density was determined by gradient column, composed of methyl iodide over bromoform. A 15 mm linear gradient was calibrated using grains of colemanite (2.42), quartz (2.65), KMnO_4 (2.70), and dolomite (2.87). Wet mineral grains around 0.2 mm across were dropped in the column and their position measured by cathetometer to ± 0.2 mm.

Density is dependent on cell volume and cell weight. The major variation in stilpnomelane cell volume results from changes in the $\text{Fe}^{2+}/\text{Fe}^{3+}$ ratio, and from variation in Mn content (see fig. 6). The major variation in cell weight results from variation in Mg content, because Si and Al are fairly constant, Mn and Fe have nearly the same mass, and alkalis and water do not vary greatly. Thus for samples of constant (Mn + Mg) (e.g. Cobar samples T, S, U, E, or the manganiferous samples C, N, O, R), density is proportional to cell

volume (fig. 7). Alternatively, the density of ferristilpnomelane (A, B, C, E, F, J, Q, U, V) is given by the relation $D = 2.89 - 0.011 \text{ Mg}$ while for ferrostilpnomelane, $D = 2.85 - 0.011 \text{ Mg}$. The figure may be some use in estimating Mg-content of stilpnomelanes, provided cell data have classified the sample as ferro-, ferri-, or mangan-stilpnomelane.

Infra-red absorption. For infra-red analysis, 2.5 mgm of sample were dispersed in 1 g of KBr, and the absorption spectrum obtained on a Pye-Unicam SP1100 spectrophotometer. In general, the results are the same as those previously published (Krautner and Medesan, 1969).

Fig. 8 shows infra-red absorption spectra between 400 and 1400 cm^{-1} for four samples of different octahedral sheet composition. The most prominent differences between them are the absorption at about 670 cm^{-1} , and the general loss of detail with increasing Fe^{3+} . The percentage absorption at 670 cm^{-1} , compared to a base absorption at either the 620 or 830 cm^{-1} transmission maxima, correlates well ($r = 0.8$) with octahedral Fe^{3+} , except for samples J and R. The shoulder at 1190 cm^{-1} on the main Si-O absorption band loses prominence with more than about 12 Fe^{3+} , and is

lost in ferristilpnomelanes. Similarly, the small absorption at 580 cm^{-1} loses prominence with increasing Fe^{3+} .

Farmer (1974) assigns absorption around 670 cm^{-1} in layer silicates to OH libration. If this assignment is correct for stilpnomelane, the progressive reduction in absorption can be correlated with loss of octahedral (OH) with increasing oxidation of Fe^{3+} .

Colour. Magnesium-poor ferrostilpnomelane is brown (S, T) becoming olive green (R, P) to pale green (J), with increasing Mg content.

Magnesium-poor ferristilpnomelane is brown-black (E, U) becoming reddish brown with increasing Mg content (B, V). Of all the samples studied here, only the shining black specimen F lives up to the name stilpnomelane.

Discussion

In order to use the graphs relating cell dimensions to composition, a and d_{001} must be deter-

mined. This is most easily done by making use of the pseudo-symmetry of stilpnomelane. All the T1 reflections can be indexed on a variety of subcells, including Gruner's monoclinic cell (1937). The simplest practice is to use an orthohexagonal cell with $a_s = \frac{1}{2}a$, $b_s = \sqrt{3} a_s$, $c_s = 3d_{001}$, index the reflections as in Table III and compute the orthohexagonal cell by least-squares refinement.

The range in a and d_{001} is such (2% and 5% respectively) that indexing by comparison with another pattern is not straightforward; for sample Z, $d_{060} = 1.563$, for sample N it is 1.596, and the difference is sufficient that the two lines might not be taken for the same reflection on a first comparison. The 060 line is always paired by the equal or slightly weaker 063 line, and gives a good approximation to b . The 009 and 0.0.12 lines are easily picked at about 4 \AA and 3 \AA respectively, but higher orders from (001) are too weak to detect. The approximate a , b , and c dimensions found from these reflections give a good guide to indexing the

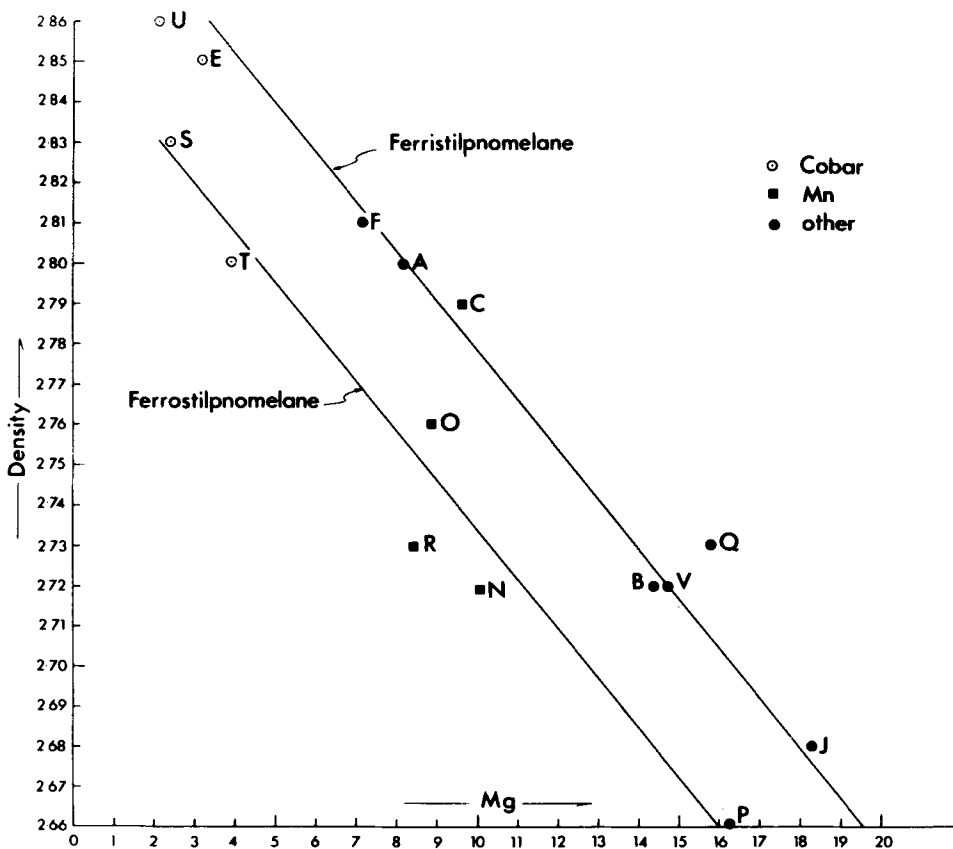


FIG. 6. Variation in density with Mg content.

other reflections, from which the cell dimensions can be obtained by least squares.

It must be remembered, however, that the orthohexagonal indexing is a convenience. There is no actual row in reciprocal space with lattice points separated by $\approx \frac{1}{36} \text{ \AA}^{-1}$ displacement parallel to c^* , and the weak T2 and T3 reflections of Parts I and II cannot be indexed on the orthohexagonal cell.

Table III lists powder diffraction (Debye-Scherrer) data for samples N, J, V, and Z, with both triclinic and orthohexagonal indices. For both indices, only one of the three superimposing lines is listed for the T1 reflections.

None of the properties of stilpnomelane examined here are indicative of any of its varied parageneses (excepting that ferristilpnomelane indicates oxidizing conditions). The possibility of a structural discontinuity between ferro- and ferristilpnomelane suggested in Part II is supported by the additional data now available and plotted in fig. 3.

The stilpnomelane structural formula is long, its unit cell large, their combination anything but memorable. Klein (1974) chose to simplify the formula by calculating to eleven oxygens. From the analyses presented here, it is recommended that any

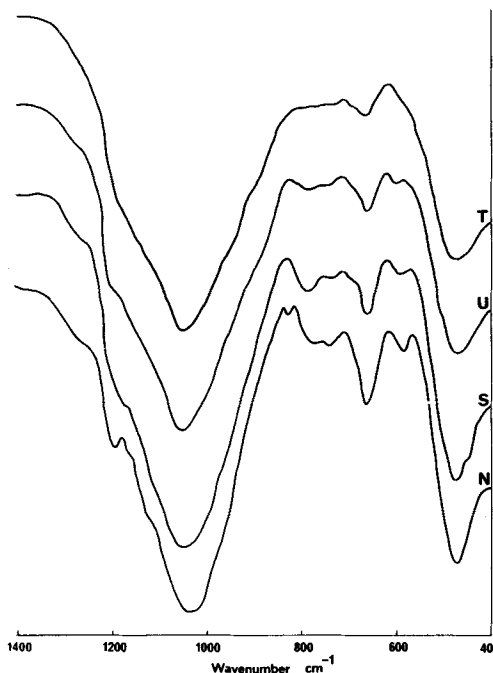


FIG. 8. Infra-red absorption spectra between 400 and 1400 cm^{-1} for four stilpnomelanes. Successive traces are displaced by 25% transmission.

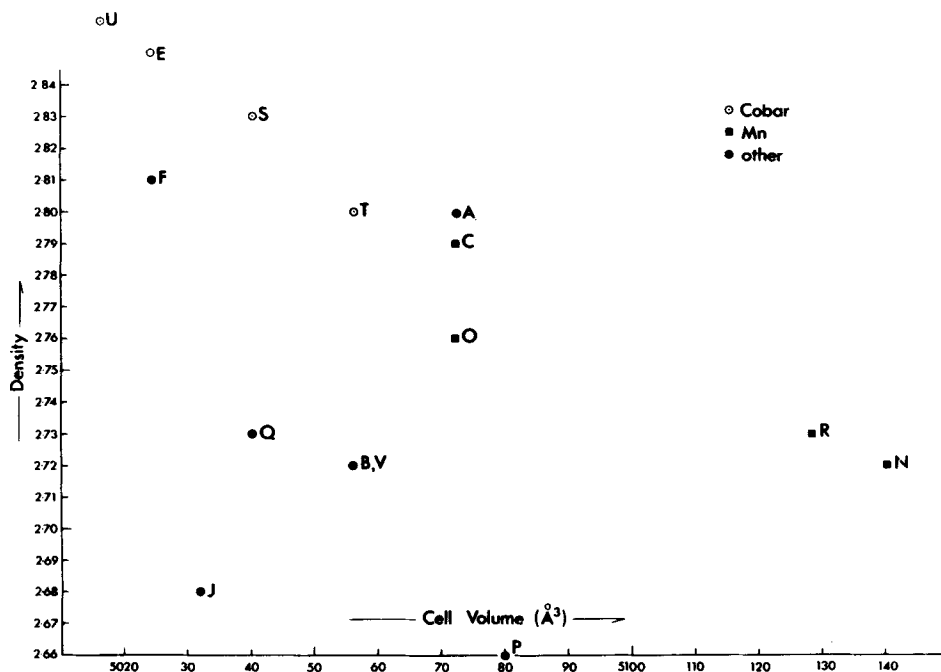


FIG. 7. Variation of density with cell volume.

simplification be division by eight, giving six octahedral cations and nine tetrahedral. An average structural formula might then approximate $K_{0.6}(Fe,Mg)_6(Si_8Al)(O,OH)_{27.2-4}H_2O$. There is no unit cell corresponding to this reduced formula;

however, an orthohexagonal cell with $a = 5.45$, $b = \sqrt{3}a$, $d_{001} = 12.2 \text{ \AA}$ has $\frac{1}{8}$ the volume of the true cell and its a and b dimensions are similar to those of other layer silicates. Because Si totals close to eight, the basis used by Gruner (1937) to calculate structural formulae and accepted by Deer *et al.* (1962) in their tabulation of analyses, reduced formulae are directly comparable with most of those already in the literature.

TABLE III. Powder diffraction data for four stilpnomelanes

Tri- clinic indices hkl	Ortho- hexa- gonal hkl	N		J		V		Z	
		I	d	I	d	I	d	I	d
001	003	10	12.4	10	12.1	10	12.4	10	12.6
102	—	1	7.21	4	6.96	—	—	—	—
002	006	4	6.07	2	6.06	2	6.16	4	6.31
222	—	2	5.51	5	5.44	3	5.42	2	5.40
242									
441	—	3	4.77	5	4.74	3	4.70	2	4.69
232	—	2	4.38	3	4.34	2	4.32	1	4.29
003	009	7	4.05	10	4.02	6	4.11	7	4.20
502	—	1	3.82	2	3.79	1	3.76	1	3.73
053									
551									
333	—	2B	3.6	5B	3.6	3B	3.6	1	3.6
363									
014									
004									
004	0.0.12	6	3.035	8	3.025	3	3.082	*	3.15
445	202	6	2.735	7	2.703	4	2.691	7	2.681
443	204	1	2.646	—	—	1	2.61	—	—
446	205	10	2.583	10	2.558	10	2.552	10	2.550
442	207	3	2.442	1	2.424	1	2.415	—	—
447	208	8	2.362	6	2.344	5	2.345	5	2.350
441	2.0.10	4	2.202	3	2.186	3	2.190	1	2.202
448	2.0.11	6	2.121	6	2.107	5	2.114	4	2.126
440	2.0.13	3	1.968	1	1.952	1	1.967	1	1.981
449	2.0.14	3	1.894	4	1.885	3	1.895	—	—
4.4.10	2.0.17	4	1.693	5	1.686	2	1.699	—	—
12.0.5	060	8	1.596	8	1.580	5	1.570	4	1.564
12.0.4	063	7	1.582	7	1.566	4	1.558	3	1.551
12.0.3	066	3	1.543	3	1.529	1	1.523	1	1.517
4.4.11	2.0.20	3	1.520	3	1.516	1	1.530	—	—
12.0.2	069	1	1.485	1	1.471	1	1.467	—	—
443	2.0.22	2	1.420	3	1.415	1	1.431	—	—
12.0.1	0.6.12	2	1.412	3	1.401	1	1.399	—	—
888	402	2	1.377	2	1.364	2	1.356	—	—
887	405	—	—	4	1.345	2	1.377	1	1.333

* Obscured by Si-standard.

N = Manganiferous ferrostilpnomelane.

J = Magnesian ferrostilpnomelane.

V = Ferristilpnomelane.

Z = Extreme ferristilpnomelane.

Acknowledgements. We are most grateful to Mr. R. S. Freeman and J. Wasik for assistance with the analyses, and for all the infra-red data. The management of Cobar Mines Pty. Ltd., kindly allowed access to drill-core, and we are particularly grateful to Mr. W. J. L. Brooke, who assisted in collecting and locating the Cobar samples.

REFERENCES

- Cremer (M. C.) and Elsheimer (H. N.), 1972. *Anal. Chim. Acta*, **60**, 183.
- Deer (W. A.), Howie (R. A.), and Zussman (J.), 1962. *Rock Forming Minerals*, **3**, Wiley.
- Eggleton (R. A.), 1972. *Mineral. Mag.* **38**, 693-711.
- 1975. *Am. Mineral.* **60**, 1063-8.
- and Bailey (S. W.), 1965. *Clay Miner. Proc. Nat. Conf.* **13**, 49.
- Farmer (V. C.), 1974. *Mineral. Soc. Monogr.* **4**.
- Graham (C. M.), 1976. *Mineral. Mag.* **40**, 467-72.
- Gruner (J. W.), 1937. *Am. Mineral.* **22**, 915-25.
- Hutton (C. O.), 1938. *Mineral. Mag.* **25**, 172-206.
- Klein (C., Jr.), 1974. *Can. Mineral.* **12**, 475-98.
- Krautner (H. G.) and Medesan (A.), 1969. *Tschermaks Mineral. Petrogr. Mitt.* ser. 3, **13**, 203.
- Matkovsky (O. I.), 1964. *Mineral. sborn. Lvov. geol. Obshch.* **18**, 59-66.
- Nitsch (K. H.), 1970. *Fortschr. Mineral.* **47**, 48-9.
- Norrish (K.) and Hutton (J. T.), 1969. *Geochim. Cosmochim. Acta*, **33**, 431-53.
- Peck (L. C.), 1964. *Bull. U.S. Geol. Surv.* **1170**.
- Rayner (E. O.), 1961. *Geol. Surv. New South Wales*, unpublished report.
- Read (P.), 1973. *Bull. Geol. Surv. Can.* **193**.
- Riley (J. P.), 1958. *Analyst*, **83**, 42-9.
- Shirozu (H.), 1964. *Rept. Fac. Sci. Kyushu Univ., Geol.* **5**, vii, 1.

[Manuscript received 12 December 1977,
revised 24 April 1978]

Table I. Chemical analyses and physical properties of stilpnomelane

	N ¹	P	W ²	R	J	S	T	O	Q	F	E	U	B ¹	V	C	A	Z ^{1,3}
SiO ₂	44.74	46.37	42.48	45.48	48.21	44.65	44.86	44.64	45.88	45.99	44.10	43.88	45.64	44.88	44.17	42.69	46.66
TiO ₂	N.D.	0.03	0.13	0.05	0.04	0.25	0.02	0.01	0.04	0.01	0.48	0.02	<0.07	0.52	0.05	0.01	0.0
Al ₂ O ₃	6.10	6.30	6.28	5.92	4.35	6.23	6.11	6.29	6.30	4.98	4.89	5.79	6.44	6.69	6.47	5.58	3.92
Fe ₂ O ₃	2.92	5.38	9.19	8.64	13.03	13.48	14.06	14.21	17.30	20.98	23.45	24.01	25.14	25.46	26.38	33.70	N.D.
FeO	24.52	20.77	19.61	18.67	14.00	22.97	22.00	14.36	9.01	12.85	14.36	14.04	3.80	2.73	3.35	0.30	32.60
MnO	4.40	0.66	3.19	4.40	0.27	0.28	0.34	4.88	0.69	0.59	0.27	0.24	0.61	0.53	3.05	2.43	0.34
MgO	5.00	8.07	4.93	4.05	9.11	1.17	1.88	4.24	7.93	3.42	1.49	1.05	7.00	7.16	4.56	3.89	4.12
CaO	<0.07	0.28	0.80	0.43	0.28	0.06	0.02	0.18	0.31	0.12	0.18	0.04	<0.07	0.79	0.58	0.13	0.56
Na ₂ O	0.30	0.13	0.00	0.73	0.06	0.95	1.08	0.03	0.00	0.42	0.97	0.77	<0.10	0.12	0.06	0.07	N.D.
K ₂ O	3.42	2.58	1.97	1.21	1.99	1.41	1.42	2.94	2.27	1.40	1.48	1.70	0.77	1.54	1.20	1.81	0.40
P ₂ O ₅	N.D.	0.00	0.51	0.13	0.00	0.05	0.00	0.00	0.00	0.00	0.09	0.00	N.D.	0.03	0.01	0.02	N.D.
CO ₂	N.D.	0.18	0.88	0.29	N.D.	0.12	0.06	0.0	0.90	0.61	0.15	0.14	N.D.	1.21	0.14	0.99	N.D.
H ₂ O	N.D.	8.87	7.65	7.30	8.46	7.27	7.50	8.03	8.28	7.32	8.01	6.55	N.D.	8.80	8.17	7.83	N.D.
S			1.73														
TOTAL	91.40	99.62	99.35	97.30	99.80	98.89	99.65	99.81	98.91	99.22	99.92	98.23	89.40	99.46	98.14	99.45	88.60
D	2.72	2.66	N.D.	2.73	2.68	2.83	2.80	2.76	2.73	2.81	2.85	2.86	2.72	2.72	2.79	2.80	N.D.
γ	1.586	1.580	1.581	~1.62	1.612	1.674	1.681	1.646	1.665	1.693	1.727	1.730	1.688	1.689	1.710	1.740	N.D.
α	22.11	22.02	22.07	22.09	21.88	21.94	21.98	21.95	21.80	21.82	21.80	21.83	21.75	21.76	21.77	21.72	21.66
d ₀₀₁	12.14	12.10	12.14	12.14	12.14	12.10	12.08	12.15	12.24	12.19	12.22	12.15	12.34	12.33	12.35	12.41	12.60
Si	62.7	62.8	61.8	63.8	65.2	63.9	63.7	62.7	63.3	65.1	63.3	62.9	62.9	61.9	62.6	60.8	65.3
Al ^{iv}	9.3	9.2	10.2	8.2	6.8	8.1	8.3	9.3	8.7	6.9	8.3	9.1	9.1	10.1	9.4	9.4	6.5
Al ^{vi}	0.8	0.9	0.6	1.6	0.1	2.4	1.9	1.1	1.5	1.4		0.7	1.4	0.8	1.4		
Fe ³⁺	3.1	5.5	7.7	9.1	13.2	14.5	15.0	15.0	18.0	22.3	25.3	25.9	26.1	26.4	28.1	36.1	38.2
Fe ²⁺	28.7	23.5	23.9	21.9	15.8	27.5	26.1	16.8	10.4	15.2	17.2	16.8	4.4	3.1	4.0	0.4	0
Mn	5.2	0.8	3.9	5.2	0.3	0.3	0.4	5.8	0.8	0.7	0.3	0.3	0.7	0.6	3.7	2.9	0.4
Mg	10.4	16.3	10.7	8.5	18.3	2.5	4.0	8.9	16.3	7.2	3.2	2.2	14.4	14.7	9.6	8.2	8.6
Ca	<0.1	0.4	0.2	0.6	0.4	0.1	0.0	0.3	0.6	0.2	0.3	0.1	<0.1	1.2	0.9	0.2	0.8
Na	0.4	0.3	-	2.0	0.2	2.6	3.0	0.1	-	1.2	2.7	2.1	<0.3	0.3	0.2	0.2	N.D.
K	6.1	4.5	3.7	2.2	3.4	2.6	2.6	5.3	4.0	2.5	2.7	3.1	1.3	2.7	2.2	3.3	0.7
OH	46.9	47.2	48.4	43.5	37.7	35.5	35.0	36.0	34.0	29.5	29.0	29.3	30.1	30.3	26.1	20.0	16.0
H ₂ O	-	16.5	-	12.5	17.6	17.0	18.0	19.6	21.1	19.5	19.4	16.8	-	23.3	25.4	-	-
ΣRV ¹	48.2	47.0	N.D.	46.3	47.7	47.2	47.4	47.6	47.0	46.8	46.0	45.9	47.0	45.6	46.8	47.6	N.D.
INTER-LAYER ⁺	6.7	5.6	4.1	5.4	4.4	5.3	5.6	6.0	5.2	4.1	6.0	5.4	~2	5.4	4.2	3.9	2.3
ANALYST	N.W.	BWC	P.B.	BWC	BWC	BWC	BWC	BWC	P.B.	BWC	BWC	BWC	N.W.	BWC	BWC	BWC	F.W.

1. Electron Microprobe analysis, except for FeO.

2. 0.67% CaO subtracted as apatite, 2.15% Fe₂O₃ subtracted as pyrite in calculating structural formula.

3. Fe reported as FeO, assumed Fe³⁺ in calculating structural formula.

Analysts: BWC: B.W. Chappell; NM: N. Mare; PB: P. Beasley; FW: F. Wilkinson.

- A. Crystal Falls, Minn., U.S.A. (see Part I)
- B. French Ridge, N.Z.
- C. Queenstown, Otago, N.Z. (cf. Hutton, 1956)
- D. Poplar Ck., B.C., Canada (Read 1973, Part II, anal. 25)
- E. Cobar, N.S.W., Australia (Rayner 1961)
- F. Cuyuna Ra., Minn., U.S.A.
- G. Cuyuna Ra., Minn., U.S.A. (Part II, anal. 18)
- H. Cuyuna Ra., Minn., U.S.A. (Part II, anal. 11)
- I. Cuyuna Ra., Minn., U.S.A. (Part II, anal. 13)
- J. Auburn Mine, Mich., U.S.A. Pale green rosettes in quartz vein.
- K. Franklin, N.J., U.S.A. (Part II, anal. 42)
- L. Queenstown, Otago, N.Z. (Part II, anal. 8)
- M. Hamersley Ra., W. Australia (Part II, anal. 1)

- N. Grythytte, Sweden. Pale green fraction
- O. Grythytte, Sweden. Brown fraction
- P. Lake Wanaka, N.Z. Green fraction
- Q. Lake Wanaka, N.Z. Brown fraction
- R. Laytonville Quarry, Mendocino Co., Calif., U.S.A.
- S. Cobar, N.S.W., Australia. D.H. CM1501, 1425'
- T. Cobar, N.S.W., Australia. D.H. CM16, 1450'
- U. Cobar, N.S.W., Australia. D.H. CM14, 585'
- V. Matukituki R. N.Z.
- W. Coast Ra., Calif. U.S.A.
- X. Cobar, N.S.W., Australia. D.H. CM13, 520'
- Y. Cobar, N.S.W., Australia. D.H. CM16, 1260'
- Z. Girilang, A.C.T., Australia.

TABLE II. Ferric iron per 48 octahedral sites for sample numbers as reported in Part II (column 2), and as predicted from refractive index and Mg content using Fe³⁺ = 213(γ-1)-616 + 0.0037 Mg (column 3)

Sample	Fe ³⁺			Sample	Fe ³⁺			Sample	Fe ³⁺		
2	2	2	14	8	7	26	19	24			
3	3	5	15	14	12	27	26	26			
6	3	5	19	20	20	28	22	26			
7	11	10	20	20	22	29	20	20			
8	3	4	21	26	23	30	27	26			
9	8	6	22	20	22	32	25	24			
10	5	9	24	21	23	34	27	29			
12	9	10	25	26	25	35	30	30			